Scattering of light from a two-dimensional array of spherical particles on a substrate

1991 J. Phys.: Condens. Matter 3 8135

(http://iopscience.iop.org/0953-8984/3/41/012)

J. Phys.: Condens. Matter 3 (1991) 8135–8148. Printed in the UK

Scattering of light from a two-dimensional array of spherical particles on a substrate

N Stefanou† and A Modinos‡

† Solid State Section, University of Athens, Panepistimioupolis, New Buildings, GR-157 71 Athens, Greece

‡ Department of Physics, National Technical University of Athens, Zografou Campus, GR-157 73 Athens, Greece

Received 1 November 1990, in final form 10 June 1991

Abstract. We present a method for the calculation of the scattering of light by a periodic two-dimensional array of spherical particles adsorbed on a uniform dielectric slab. Multiple scattering of light between the particles of the overlayer and between the overlayer and the substrate is taken fully into account. The method is applied to light scattering from a square lattice of gold particles on a sapphire substrate for which experimental data are available. The agreement between theory and experiment is reasonably good.

1. Introduction

The study of optical properties of inhomogeneous films has attracted special interest in the last few years for physical as well as for technological reasons. The Raman scattering by molecules adsorbed on rough metal surfaces for instance has drawn much attention due to the extremely large enhancement of the scattering cross section. The understanding of the origin of the surface-enhanced Raman scattering provided the impetus for a number of optical investigations of rough surfaces [1–4]. Thin films consisting of small metallic particles embedded in a dielectric host material have remarkable optical properties which might be useful for specific technological purposes, e.g. as coatings for solar energy absorbers [5]. In general, granular or discontinuous metal films can exhibit optical properties which are strikingly different from the bulk behaviour and have been for many years the active target of experimental investigation [6, 7]. Recently, Craighead and Niklasson [8] and Niklasson and Craighead [9] fabricated two-dimensional square arrays of gold particles having diameters of 20–35 nm with a spacing of 50 nm on thick sapphire substrates and measured the optical transmission through this structure.

From a theoretical point of view, the problem of light scattering by a spherical object situated in a homogeneous medium has been solved rigorously early in this century in terms of classical electromagnetic theory by Mie [10] and Debye [11]. In this treatment, the spheres are assumed to be large enough for the macroscopic dielectric theory to be applicable, with no other limitation on their size. When the wavelength of light is much larger than the dimension of the particles and the distance between them, the electrostatic approximation can be employed and the optical properties of the metal particles can be characterized by an effective medium, as described by Maxwell Garnett [12] for spherical particles and by David [13] for spheroidal particles. Calculations dealing with certain aspects of the optical properties of inhomogeneous systems consisting of metallic spheres of radius 10 nm or so in a dielectric host have been published by a number of workers [14–18]. Essentially, in these calculations the metal spheres are replaced by interacting dipoles with a polarizability evaluated on the basis of the Drude formula for the dielectric constant of the metal. An effective dielectric constant for the composite medium is then obtained by the use of the Clausius–Mossotti equation, or by some extension of this formula which takes into account the influence of the local electric field due to the randomly distributed particles [14]. Vlieger and co-workers [19–24] developed a statistical theory for the dielectric properties of two-dimensional systems of spherical, truncated spherical or spheroidal particles on a substrate, which takes into account particle–substrate interaction by the method of image multipoles. The boundary conditions for the potential and the normal component of the displacement vector yield an infinite set of inhomogeneous linear equations for the multipole coefficients, which can be solved approximately by considering a large enough finite set of equations corresponding to a finite number of multipoles. The above-mentioned methods cannot be employed when the interparticle distance and (or) the size of the particles become(s) comparable with the wavelength of the incident radiation. Moreover, even when the interparticle distance is much smaller than the wavelength of the incident light, replacement of the metal particles by dipoles is not realistic when the fractional volume occupied by these spheres is larger than 0.5 or so. At higher concentrations, multiple interactions must be taken into account [25, 26].

There are substances which form periodic lattices just as ordinary solids but have lattice constants comparable with the wavelengths of ultraviolet or visible light. For example, there are ordered structures of some polymers [27–30], void lattices in ion- or neutron-bombarded metals [31–33], and ordered structures in some biological systems [34]. These systems therefore make the diffraction of electromagnetic waves in the ultraviolet and visible range possible. A proper description of such phenomena should take into account the multiple scattering of the electromagnetic field between the particles within the inhomogeneous substance.

Lamb *et al* [35] proposed a modified version of the Korringa–Kohn–Rostoker (KKR) method, used in the calculation of the energy band structure of electrons in solids [36, 37], to evaluate the field incident on a given metal sphere due to the waves scattering from all other spheres in the composite medium. Their theory yields an effective propagation wavevector in the infinite crystal (corrections due to disorder are included for some limiting cases) and as such is related to a transmission experiment in the forward direction but it does not describe an actual experiment because it does not allow for a proper matching of the incident electromagnetic wave to the reflected and transmitted into the 'crystal' waves at the interface. Ohtaka and co-workers [38–41] also transferred multiple-scattering techniques from the KKR band-structure method and the low-energy electron diffraction (LEED) theory [42] to the problem of multiple scattering of classical waves. Recently, Modinos [43] developed a formalism for multiple scattering of electromagnetic waves by a periodic monolayer of spheres using a straightforward approach based entirely on electromagnetic theory. This method is equivalent to that of Ohtaka [39] and has all the advantages of the LEED theory. It can describe the physical situation in an actual transmission experiment, i.e. it makes it possible to calculate the reflection and transmission matrix elements, for light incident at a given angle, of a two-dimensional array of spherical particles embedded in a dielectric host material. The reflection and transmission matrix elements of multilayers can be obtained as in the case of electron scattering from knowledge of the scattering matrix elements of the constituent monolayers.

In this paper we develop the formalism of [43] further by pointing out certain symmetries in the matrix elements which describe the multiple scattering of light by a plane of spheres (section 2.1) and incorporate into the formalism the influence of the substrate (section 2.2). Finally, we present numerical applications of the method to transmission experiments (section 3).

2. Formalism

2.1. Scattering of electromagnetic waves by a two-dimensional ordered array of spheres

In a medium characterized by a complex frequency-dependent permittivity $\varepsilon(\omega)$ the electric field $\boldsymbol{E}(\boldsymbol{r}, t) = \mathrm{Re}[\tilde{\boldsymbol{E}}(\boldsymbol{r}) \exp(-\mathrm{i}\omega t)]$ can be expanded in spherical waves as follows [44]:

$$\tilde{\boldsymbol{E}}(\boldsymbol{r}) = \sum_{l=1}^{\infty} \sum_{m=-l}^{l} \left(\frac{\mathrm{i}}{k} a_{lm}^{E} \boldsymbol{\nabla} \times z_l(kr) \boldsymbol{X}_{lm}(\hat{\boldsymbol{r}}) + a_{lm}^{H} z_l(kr) \boldsymbol{X}_{lm}(\hat{\boldsymbol{r}}) \right). \tag{1}$$

The corresponding formula for the associated magnetic field is obtained from equation (1) by interchanging the superscripts E and H, changing the sign of the factor i/k and multiplying the resulting expression by $(\varepsilon/\mu_0)^{1/2}$. We assume that the magnetic permeability equals that of vacuum μ_0. For magnetic materials, μ_0 must be replaced by μ in the relevant formulae. $k = (\mu_0 \varepsilon)^{1/2}\omega$ is the wavenumber. The functions $z_l(kr)$ may be any linear combination of the spherical Bessel function $j_l(kr)$ and the spherical Hankel function $h_l^+(kr)$. These quantities as well as $\boldsymbol{X}_{lm}(\hat{\boldsymbol{r}})$ are defined in [43]. The coefficients $a_{lm}^{E(H)}$ in equation (1) are constants to be determined.

A plane electromagnetic wave described by

$$\tilde{\boldsymbol{E}}(\boldsymbol{r}) = \tilde{\boldsymbol{E}}_0(\boldsymbol{k}) \exp(\mathrm{i}\boldsymbol{k} \cdot \boldsymbol{r}) \qquad \tilde{\boldsymbol{H}}(\boldsymbol{r}) = -(\mathrm{i}/\omega\mu_0) \boldsymbol{\nabla} \times \tilde{\boldsymbol{E}}(\boldsymbol{r}) \tag{2}$$

where $\boldsymbol{E}_0(\boldsymbol{k}) \equiv E_0(\boldsymbol{k})\boldsymbol{p}$ specifies the magnitude E_0 and the polarization $\boldsymbol{p}$ of the electric field, has a corresponding spherical wave expansion given by equation (1) with $z_l(kr) = j_l(kr)$. Writing the expansion coefficients in the form

$$a_{lm}^{0E(H)} \equiv \boldsymbol{A}_{lm}^{0E(H)} \cdot \boldsymbol{E}_0 \tag{3}$$

we can obtain explicit expressions for $\boldsymbol{A}_{lm}^{0E(H)}$ by substituting equations (2) into equation (1) and expanding $\exp(\mathrm{i}\boldsymbol{k} \cdot \boldsymbol{r})$ into spherical waves.

When the electromagnetic wave described by equations (2) is scattered by a sphere of radius S and permittivity $\varepsilon_m(\omega)$ centred at the origin of coordinates, it gives rise to a total wave field outside the sphere, composed by the incident and scattered waves. The expansion coefficients $a_{lm}^{+E(H)}$ of the scattered wave are

$$a_{lm}^{+E(H)} = T_l^{E(H)} a_{lm}^{0E(H)}. \tag{4}$$

Explicit expressions for $T_l^{E(H)}$ are given in [43].

The energy absorbed per unit time by the sphere is given by the negative integral of the Poynting vector over the surface of the sphere. We denote the average of this quantity over a period $T = 2\pi/\omega$ by $\bar{W}$. In the long-wavelength limit ($k_\mathrm{M}S$, $kS \ll 1$), one obtains the electrostatic approximation

$$\bar{W} = (4\pi\varepsilon\omega S^3/2)\, |E_0|^2\, \mathrm{Im}[(\varepsilon_\mathrm{M} - \varepsilon)/(2\varepsilon + \varepsilon_\mathrm{M})]. \tag{5}$$

We now consider an assembly of non-overlapping spheres of radius S and permittivity

$\varepsilon_{\mathrm{M}}(\omega)$, centred on the sites $\boldsymbol{R}_n$ of a two-dimensional lattice in the x–y plane, embedded in a medium of permittivity $\varepsilon(\omega)$. A plane electromagnetic wave with $\boldsymbol{k} = (\boldsymbol{k}_\parallel, k_z)$, where $\boldsymbol{k}_\parallel = (k_x, k_y)$ denotes the components of the wavevector in the plane of the spheres and k_z its component normal to this plane, is incident on the spheres from the left ($k_z > 0$). Because of the two-dimensional periodicity of the structure under consideration the corresponding scattered wave can be written as

$$\tilde{\boldsymbol{E}}_{\mathrm{sc}}(\boldsymbol{r}) = \sum_{l=1}^{\infty}\sum_{m=-l}^{l}\left(\frac{\mathrm{i}}{k} b_{lm}^{+E}\nabla \times \sum_{\boldsymbol{R}_n} \exp(\mathrm{i}\boldsymbol{k}_\parallel \cdot \boldsymbol{R}_n) h_l^+(kr_n)\boldsymbol{X}_{lm}(\hat{\boldsymbol{r}}_n) + b_{lm}^{+H}\sum_{\boldsymbol{R}_n}\exp(\mathrm{i}\boldsymbol{k}_\parallel \cdot \boldsymbol{R}_n) h_l^+(kr_n)\boldsymbol{X}_{lm}(\hat{\boldsymbol{r}}_n)\right) \tag{6}$$

where $\boldsymbol{r}_n \equiv \boldsymbol{r} - \boldsymbol{R}_n$ and $b_{lm}^{+E(H)}$ are coefficients to be determined. The scattered wave can also be expressed as a series of plane waves with wavevectors

$$\boldsymbol{K}_{\boldsymbol{g}}^{s} \equiv (\boldsymbol{k}_\parallel + \boldsymbol{g}, \pm[k^2 - (\boldsymbol{k}_\parallel + \boldsymbol{g})^2]^{1/2}) \tag{7}$$

where $\boldsymbol{k}_\parallel$ now stands for the reduced wavevector within the surface Brillouin zone of the given lattice corresponding to the incident wavevector and $\boldsymbol{g}$ are the reciprocal (two-dimensional) lattice vectors. The $s = +$ and $-$ signs on $\boldsymbol{K}$ are used for $z > 0$ and $z < 0$, respectively. Finally, we can express the amplitude of a scattered plane wave in terms of that of the incident plane wave:

$$[E_{\mathrm{sc}}]_{\boldsymbol{g}i}^{s} = \sum_{\boldsymbol{g}',i'} M_{\boldsymbol{g}i;\boldsymbol{g}'i'}^{ss'}[E_{\mathrm{in}}]_{\boldsymbol{g}'i'}^{s'} \tag{8}$$

where the subscripts i and i' denote Cartesian components.

$$M_{\boldsymbol{g}i;\boldsymbol{g}'i'}^{ss'} = \delta_{ss'}\delta_{\boldsymbol{g}\boldsymbol{g}'}\delta_{ii'} + [\mathbf{A}_{\boldsymbol{g}i}^{s}]^{\mathrm{T}}\mathbf{B}_{\boldsymbol{g}'i'}^{+Hs'} - \frac{1}{k}\sum_{j,j'}\varepsilon_{ij'j}K_{\boldsymbol{g}j}^{s}[\mathbf{A}_{\boldsymbol{g}j'}^{s}]^{\mathrm{T}}\mathbf{B}_{\boldsymbol{g}'i'}^{+Es'}. \tag{9}$$

The superscript T denotes as usual the transpose matrix and

$$\varepsilon_{ijk} \equiv \begin{cases} 0 & \text{when any two of the indices are equal} \\ 1 & \text{if } i, j, k \text{ is an even permutation of } x, y, z \\ -1 & \text{if } i, j, k \text{ is an odd permutation of } x, y, z. \end{cases}$$

In equation (9) we used, for convenience, matrix notation in angular momentum space. Explicit expressions for the column vector $\mathbf{A}_{\boldsymbol{g}i}^{s} \equiv \{A_{lm}(\boldsymbol{K}_{\boldsymbol{g}}^{s})\}_i$ are given in [43]. $\mathbf{B}_{\boldsymbol{g}i}^{+E(H)} \equiv \{b_{lm}^{+E(H)}\}$ are to be evaluated for an incident plane wave with parallel wavevector $\boldsymbol{k}_\parallel + \boldsymbol{g}$ incident from the left (right) corresponding to $s = +$ $(-)$ with an ith component electric field. The above quantities enter the calculation through the A^0-coefficients defined by equations (3), which we may write as the column matrix $\mathbf{A}_{\boldsymbol{g}i}^{0E(H)s} \equiv \{A_{lm}^{0E(H)}(\boldsymbol{K}_{\boldsymbol{g}}^{s})\}_i$. We have

$$\begin{pmatrix} \mathbf{I} - \mathbf{T}^{E}\boldsymbol{\Omega}^{(1)} & \mathbf{T}^{E}\boldsymbol{\Omega}^{(2)} \\ -\mathbf{T}^{H}\boldsymbol{\Omega}^{(2)} & \mathbf{I} - \mathbf{T}^{H}\boldsymbol{\Omega}^{(1)} \end{pmatrix}\begin{pmatrix} \mathbf{B}^{+E} \\ \mathbf{B}^{+H} \end{pmatrix}_{\boldsymbol{g}i}^{s} = \begin{pmatrix} \mathbf{T}^{E}\,\mathbf{A}^{0E} \\ \mathbf{T}^{H}\,\mathbf{A}^{0H} \end{pmatrix}_{\boldsymbol{g}i}^{s} \tag{10}$$

where $\mathbf{I}$ is the unit matrix. The matrix elements of $\boldsymbol{\Omega}^{(1)}$ and $\boldsymbol{\Omega}^{(2)}$ depend on the scattering properties of the individual sphere and the geometry of the plane. Analytic expressions for these matrix elements are given in the appendix.

Equations (10) constitute a system of infinitely many linear equations. It is solved by introducing an angular momentum cut-off $l_{\max}$ and truncating all angular momentum

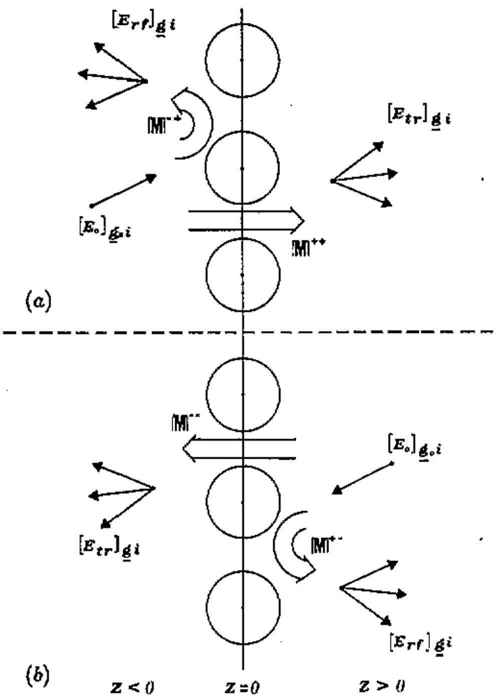

Figure 1. Scattering of a plane wave from a periodic monolayer of spherical particles: (*a*) plane wave incident from the left; (*b*) plane wave incident from the right.

expansions to $l_{\max}$, thus reducing the dimension of the system to $2\{(l_{\max}+1)^2-1\}$. One can easily show using the properties of $\mathbf{\Omega}^{(1)}$ and $\mathbf{\Omega}^{(2)}$ given in the appendix that this system can be reduced to two systems of $(l_{\max}+1)^2-1$ linear equations. This can be achieved if we split the angular momentum space into two subspaces with $l+m$ odd and $l+m$ even. Substituting the expression for $\mathbf{A}^s_{gi}$ derived in [43] into equation (9) and using the fact that the B^+-coefficients couple only to certain of the A^0-coefficients, one can show that the matrices $\mathbf{M}$ obey the following symmetry relations:

$$M^{ss'}_{gi;g'i'} = M^{-s-s'}_{gi;g'i'} \qquad M^{ss'}_{gi;g'i'} = -M^{-s-s'}_{gi;g'i'} \tag{11}$$

for the combinations $(i,i') = (x,x), (y,y), (z,z), (x,y), (y,x)$ and $(i,i') = (x,z), (z,x), (y,z), (z,y)$ respectively.

For a wave incident from the left the components of the transmitted and reflected electric field are given by (see also figure 1)

$$[E_{\mathrm{tr}}]_{gi} = \sum_{g',i'} M^{++}_{gi;g'i'}[E_{\mathrm{in}}]^+_{g'i'} \tag{12}$$

$$[E_{\mathrm{rf}}]_{gi} = \sum_{g',i'} M^{-+}_{gi;g'i'}[E_{\mathrm{in}}]^+_{g'i'}. \tag{13}$$

The transmittance $\mathcal{T}$ and reflectivity $\mathcal{R}$ are defined as the ratios of the fluxes of the transmitted and reflected waves respectively to the flux of the incident wave. Integrating the Poynting vector over the x–y plane from both sides of the layer and taking the average over a period, one can show that

$$\mathcal{T}(\mathcal{R}) = \sum_{g,i}[E_{\mathrm{tr(rf)}}]_{gi}[E_{\mathrm{tr(rf)}}]^*_{gi}K^+_{gz}\Big/\sum_{g,i}[E_{\mathrm{in}}]_{gi}[E_{\mathrm{in}}]^*_{gi}K^+_{gz}. \tag{14}$$

The requirement for energy conservation implies that the absorbance $\mathcal{U}$ of the periodic monolayer of spheres is

$$\mathcal{U} = 1-\mathcal{T}-\mathcal{R}. \tag{15}$$

2.2. Influence of the substrate

Let the substrate be a homogeneous dielectric plate of permittivity ε_s embedded in a medium of permittivity ε, the interfaces being the plane surfaces $z = l$ and $z = l + d$. Assume that the incident electromagnetic field is a plane wave, given by equations (2) with the wavevector K_g^+ in the x–z plane. The normal to the interfaces components of the wavevector inside and outside the substrate are

$$q_s = [\varepsilon_s \mu_0 \omega^2 - (k_\parallel + g_0)^2]^{1/2} \tag{16}$$

and

$$q = [\varepsilon \mu_0 \omega^2 - (k_\parallel + g_0)^2]^{1/2} \tag{17}$$

respectively. The boundary conditions for continuity of the tangential components of the electric and magnetic fields at the interfaces determine the transmitted and reflected electric field as follows:

$$[E_{\mathrm{tr}}]_{gi} = T^0_{gi}\{E_0(K^+_{g0})\}_i \delta_{gg0} \tag{18a}$$

$$\{\tilde{E}_{\mathrm{tr}}(r)\}_i = \exp[\mathrm{i}K^+_{g0}\cdot(r - R)]\,[E_{\mathrm{tr}}]_{g0i} \tag{18b}$$

$$[E_{\mathrm{rf}}]_{gi} = R^0_{gi}\{E_0(K^+_{g0})\}_i \delta_{gg0} \tag{19a}$$

$$\{\tilde{E}_{\mathrm{rf}}(r)\}_i = \exp(\mathrm{i}K^-_{g0}\cdot r)\,[E_{\mathrm{rf}}]_{g0i} \tag{19b}$$

where

$$T^0_{g0i} = \exp(\mathrm{i}ql)\,\{b_i c_i \exp(\mathrm{i}q_s d)/[1 - a_i^2 \exp(2\mathrm{i}q_s d)]\} \tag{20}$$

$$R^0_{g0i} = \exp(2\mathrm{i}ql)\,\{a_i b_i c_i \exp(2\mathrm{i}q_s d)/[1 - a_i^2 \exp(2\mathrm{i}q_s d)] - a_i\} \tag{21}$$

with

$$a_x = (\varepsilon_s q - \varepsilon q_s)/(\varepsilon_s q + \varepsilon q_s) \qquad b_x = 1 - a_x \qquad c_x = 1 + a_x \tag{22a}$$

$$a_y = (q_s - q)/(q_s + q) \qquad b_y = 1 - a_y \qquad c_y = 1 + a_y \tag{22b}$$

$$a_z = -a_x \qquad b_z = 2\varepsilon q/(\varepsilon_s q + \varepsilon q_s) \qquad c_z = 2\varepsilon_s q_s/(\varepsilon_s q + \varepsilon q_s) \tag{22c}$$

and $R \equiv (0, 0, d + l)$.

If the parallel to the interfaces component of the wavevector of the incident field makes an angle φ with the x axis, we define the transmission matrix $\mathbf{T}$ as

$$T_{gx;g'x} = \delta_{gg'}(T^0_{gx}\cos^2\varphi + T^0_{gy}\sin^2\varphi) \tag{23a}$$

$$T_{gy;g'y} = \delta_{gg'}(T^0_{gx}\sin^2\varphi + T^0_{gy}\cos^2\varphi) \tag{23b}$$

$$T_{gz;g'z} = \delta_{gg'}T^0_{gz} \tag{23c}$$

$$T_{gx;g'y} = T_{gy;g'x} = \delta_{gg'}(T^0_{gx} - T^0_{gy})\sin\varphi\cos\varphi \tag{23d}$$

$$T_{gx;g'z} = T_{gz;g'x} = T_{gy;g'z} = T_{gz;g'y} = 0 \tag{23e}$$

with an exactly analogous definition for the reflection matrix $\mathbf{R}$. In this case, the transmitted and reflected electric field are given by

$$[E_{\mathrm{tr}}]_{gi} = \sum_{i'} T_{gi;gi'}\{E_0(K^+_{g0})\}_{i'}\delta_{gg0} \tag{24a}$$

$$\{\tilde{E}_{\mathrm{tr}}(r)\}_i = \exp[\mathrm{i}K^+_{g0}\cdot(r - R)]\,[E_{\mathrm{tr}}]_{g0i} \tag{24b}$$

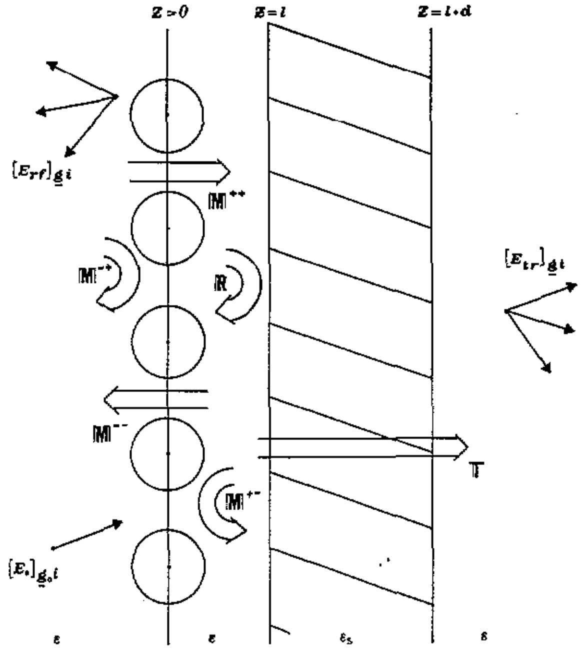

Figure 2. Scattering of a plane wave from a periodic monolayer of spherical particles on a substrate.

$$[E_{\rm rf}]_{gi} = \sum_{i'} R_{gi;gi'}\{E_0(K^+_{g0})\}_{i'}\,\delta_{gg_0} \tag{25a}$$

$$\{\tilde{E}_{\rm rf}(r)\}_i = \exp({\rm i}K^-_{g_0}\cdot r)\,[E_{\rm rf}]_{g_0 i}. \tag{25b}$$

Finally, we consider a system consisting of a periodic monolayer of spheres at the plane $z=0$ and a substrate. The transmittance and reflectivity of this system can be expressed in terms of the scattering matrices $\mathbf{M}^{ss'}$ of the coating layer, given by equation (9), and the transmission and reflection matrices, $\mathbf{T}$ and $\mathbf{R}$ respectively, of the substrate, derived above. The situation is schematically illustrated in figure 2. For an incident plane wave with wavevector $K^+_{g_0}$, we obtain after some straightforward algebra the following formulae for the transmitted and reflected electric field:

$$[E_{\rm tr}]_{gi} = \sum_{i'} \{\mathbf{T}(\mathbf{I}-\mathbf{M}^{+-}\mathbf{R})^{-1}\mathbf{M}^{++}\}_{gi;g_0 i'}\{E_0(K^+_{g0})\}_{i'} \tag{26a}$$

$$\{\tilde{E}_{\rm tr}(r)\}_i = \sum_g \exp[{\rm i}K^+_g\cdot(r-R)]\,[E_{\rm tr}]_{gi} \tag{26b}$$

$$[E_{\rm rf}]_{gi} = \sum_{i'} \{\mathbf{M}^{-+}+\mathbf{M}^{--}\mathbf{R}(\mathbf{I}-\mathbf{M}^{+-}\mathbf{R})^{-1}\mathbf{M}^{++}\}_{gi;g_0 i'}\{E_0(K^+_{g0})\}_{i'} \tag{27a}$$

$$\{\tilde{E}_{\rm rf}(r)\}_i = \sum_g \exp({\rm i}K^-_g\cdot r)[E_{\rm rf}]_{gi}. \tag{27b}$$

The transmittance and reflectivity of the system are obtained by substitution of equations (26) and (27) in equations (14).

3. Applications

3.1. Scattering from a periodic monolayer of dielectric spheres

In this section we calculate the reflection and transmittance of electromagnetic waves from a periodic monolayer of dielectric spheres. In order to test our method and compare

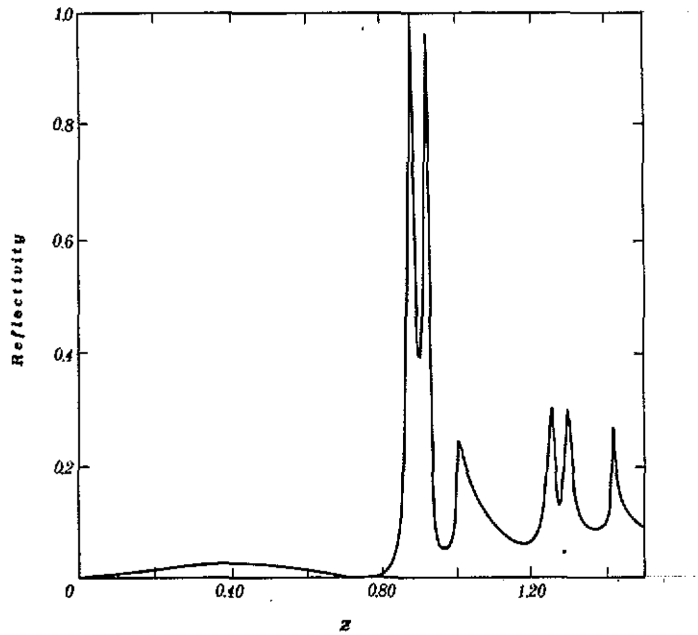

Figure 3. Reflectivity of normally incident light of reduced wavenumber Z from a square lattice of polystyrene spheres in water. The ratio of the sphere radius to the lattice parameter is equal to 0.35.

it with that of Ohtaka and co-workers [38–41], we first consider a physical system that they treated in some detail: a monolayer of spherical polystyrene particles in water [41]. The spherical particles of radius $S = 35$ nm are arranged on a two-dimensional square lattice with a lattice constant $a = 100$ nm. For the relative refractive index we use the value corresponding to polystyrene particles in water in the visible range: $(\varepsilon_M/\varepsilon)^{1/2} = 1.6$.

In figure 3 we present our results for the reflectivity of normally incident x-polarized light as a function of the reduced wavenumber $Z = ka/2\pi$. We performed the calculation using an angular momentum cut-off $l_{max} = 6$, which is sufficient to obtain well converged results in the entire considered range of Z. For values of Z given by $0 \leqslant Z < 1$, only the first reciprocal lattice vector $g_0 = 2\pi(0, 0)/a$ enters in the calculation of the reflectivity and the transmittance of the system. For $1 \leqslant Z < \sqrt{2}$ the next four vectors ($g_1 = 2\pi(1, 0)/a$, $2\pi(-1, 0)/a$, $2\pi(0, 1)/a$, $2\pi(0, -1)/a$) must be included whereas, for $\sqrt{2} \leqslant Z < 2$, one must take into account also the reciprocal lattice vectors: $g_2 = 2\pi(1, 1)/a, 2\pi(1, -1)/a, 2\pi(-1, 1)/a, 2\pi(-1, -1)/a$. Comparison with the results of Inoue *et al* [41] shows that there is overall agreement in the characteristic features of the reflectivity curve. These features have been extensively discussed by Inoue *et al* [41]. We find a double peak at $Z = 0.88$ and $Z = 0.92$, of height almost equal to one and a lower peak at $Z = 1$, all these in perfect agreement with the results of Inoue *et al*. We also find a second smaller double peak at $Z = 1.25$ and $Z = 1.29$ that is similarly produced by Inoue *et al* at the same positions but with a somewhat smaller magnitude. The last peak at $Z = \sqrt{2}$ is not produced in the reflectivity curve of Inoue *et al*. We believe, however, that this peak is indeed there.

Table 1 shows the convergence behaviour of our results for the transmittance, as a function of the angular momentum cut-off l_{max}, for various values of both Z and the ratio

Table 1. Transmittance of a system of polystyrene spheres of radius S arranged on a square lattice of lattice parameter a in water, for normally incident light. The convergence is shown as a function of the angular momentum cut-off l_{max} for various values of the ratio S/a and the reduced wavenumber Z.

Z	l_{max}	$S/a = 0.30$	$S/a = 0.35$	$S/a = 0.40$
0.2	1	0.994 656	0.987 766	0.971 361
0.2	2	0.994 797	0.987 244	0.972 738
0.2	3	0.994 794	0.987 219	0.972 564
0.2	4	0.994 794	0.987 219	0.972 562
0.2	5	0.994 794	0.987 219	0.972 561
0.2	6	0.994 794	0.987 219	0.972 561
0.9	1	0.999 924	0.063 242	0.008 425
0.9	2	0.999 958	0.639 551	0.868 885
0.9	3	0.999 810	0.611 281	0.976 547
0.9	4	0.999 828	0.611 717	0.975 546
0.9	5	0.999 826	0.611 147	0.975 906
0.9	6	0.999 826	0.611 160	0.975 857
1.4	1	0.993 937	0.994 786	0.995 966
1.4	2	0.955 727	0.908 889	0.949 588
1.4	3	0.969 900	0.861 168	0.473 914
1.4	4	0.973 816	0.898 310	0.551 328
1.4	5	0.973 667	0.895 852	0.612 930
1.4	6	0.973 669	0.895 855	0.615 346

S/a. In the long-wavelength limit, as expected, the convergence is very fast and already the dipole term gives very good results. However, when the wavelength decreases and (or) the size of the spheres increases, higher-angular-momentum components must be taken into account in order to describe correctly both the Mie scattering from a single sphere and the multiple-scattering effects.

After calculating independently the transmittance and reflectivity of the system using equations (14) we deduced the absorbance $\mathcal{U} = 1 - \mathcal{T} - \mathfrak{R}$ which never exceeded 10^{-15}. This order of magnitude gives an indication of the numerical accuracy in our calculation, since the absorbance of a system of dielectric particles having real dielectric constants is identically zero. This result was confirmed for all the cut-offs $l_{max} = 1, 2, \ldots, 6$ that we considered in the angular momentum expansions, indicating the inherent consistency of our formalism.

3.2. *Light scattering from a square lattice of gold particles on a sapphire substrate*

We applied our method to an optical transmission experiment performed in [8, 9] on a system of gold particles arranged on a square lattice on a sapphire substrate. Despite the small deviations from periodicity and spherical shape of the particles (their axial ratio was estimated to be 1.3–1.7) occurring in the actual experiment, we have assumed in our calculations spherical particles arranged on a perfectly periodic square lattice. The diameter of the gold particles in the experiment ranged from 20 to 35 nm, whereas the lattice constant was 50 nm.

For the bulk relative dielectric function $\chi_B(\omega)$ of gold, we interpolate to the values measured by Johnson and Christy [45]. However, these values which contain both the Drude term and the interband absorption contribution must be corrected because of the

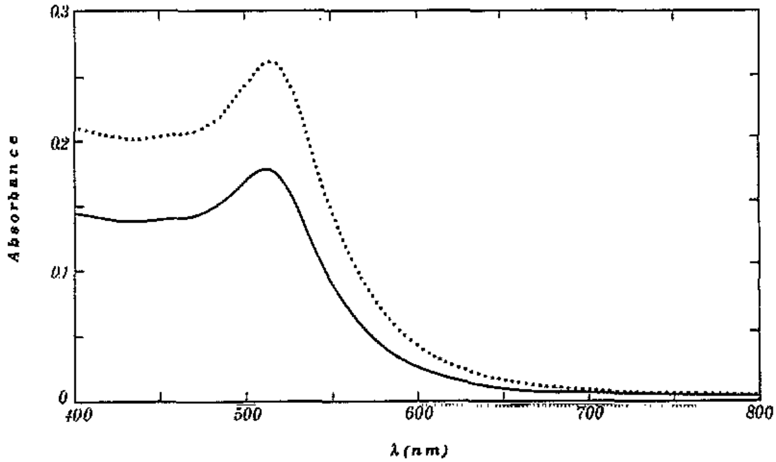

Figure 4. Absorbance of normally incident light of wavelength λ from a square lattice of Au spheres of radius $S = 15$ nm (———) and $S = 17$ nm (. . . .), in vacuum. The lattice constant is equal to 50 nm.

small size of the particles that we have. It is accepted that in small particles the electronic mean free path is shorter than in the bulk. Following several workers [6, 7, 22, 23], we incorporate this effect in the dielectric constant in an empirical manner as follows:

$$\chi(\omega) = \chi_{\rm B}(\omega) + \omega_{\rm p}^2/(\omega^2 + {\rm i}\omega\tau_{\rm B}^{-1}) - \omega_{\rm p}^2/(\omega^2 + {\rm i}\omega\tau^{-1}) \tag{28}$$

where $\omega_{\rm p}$ is the plasma frequency, $\tau_{\rm B}$ the relaxation time in the bulk metal and

$$\tau^{-1} = \tau_{\rm B}^{-1} + V_{\rm F}S^{-1} \tag{29}$$

is the inverse relaxation time, corrected for the finite size of the particle. $V_{\rm F}$ is the Fermi velocity and S the radius of the spherical particle. Following [22, 23], we use the values $\hbar\omega_{\rm p} = 8.99$ eV, $\hbar\tau_{\rm B}^{-1} = 0.027$ eV and $\hbar V_{\rm F} = 0.903$ eV nm. The refractive index of sapphire shows little dispersion in the optical region but for simplicity we use the value $n_{\rm s} = 1.77$ throughout. For the ambient we take $n = 1$.

The absorbance of the whole system (coating plus substrate) is due to the assembly of Au spheres. Thus, if we consider dielectric, instead of metallic, spheres the total absorbance must be identically zero. This is a way to check the accuracy in the calculation of total reflectivity and transmittance, given by equations (14), (15), (26) and (27). We performed this test by putting polystyrene spheres on the sapphire substrate and the total absorbance of the system was found to be 10^{-14}.

We first consider a layer of gold spheres in isolation. The calculated absorbance for two sizes of spheres (within the range of measured radii) is shown in figure 4. The most striking feature is the absorption peak at about 512 nm, which becomes more pronounced when the spheres are larger. This peak corresponds to the localized plasmon resonance of a single Au sphere as can be seen in figure 5. We confirmed that, within the range of wavelengths considered, the electrostatic limit constitutes a reasonably good approximation which in turn justifies the method used by Vlieger and co-workers [19–24] in this instance. However, this is not generally true. Calculations on silver spheres of radii of the order of 40 nm show that multiple-scattering effects produce variations in the absorption curve (shifts in the absorption peaks), which depend strongly on the lattice constant. In all our calculations we used an angular momentum cut-off $l_{\rm max} = 4$, which yields well converged results.

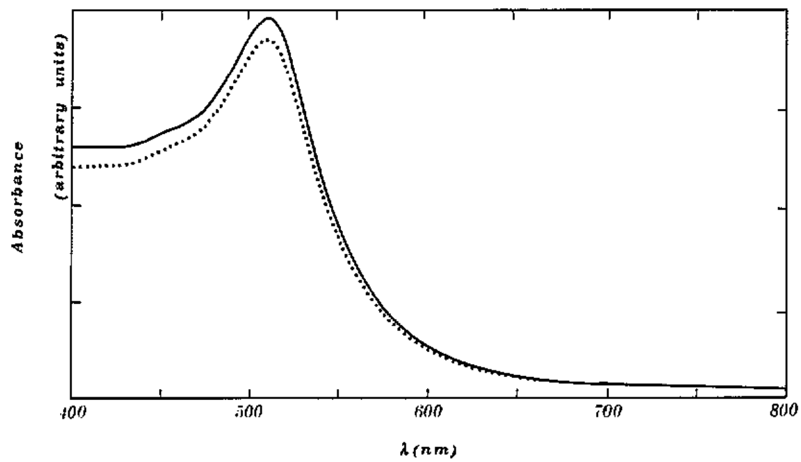

Figure 5. Absorbance of light of wavelength λ from a single Au sphere of radius $S =$ 15 nm: ———, multiple treatment; . . . . , electrostatic limit, calculated using equation (5).

If we consider the substrate alone to be a homogeneous dielectric sapphire plate, the transmittance shows a periodic oscillatory behaviour as a function of the thickness of the slab with a period equal to $\lambda/2n_s \cos\theta$ as expected. Analogous oscillatory behaviour is found for the transmittance through the coated substrate, as well as the relative transmittance with respect to that of the bare substrate. In figure 6 we show the relative transmittance averaged over a period, together with the transmittance of the coating alone, as well as the experimental data in [8, 9]. Clearly visible is the plasmon resonance peak that we calculate around $\lambda = 512$ nm. As we can see, the relative transmittance curve is shifted to higher transmittance values with respect to the transmittance of the coating alone. The calculated curve approaches the experimental curve for sphere radii ranged between 15 and 17 nm which corresponds well to the average size of particles measured in [8, 9]. The main discrepancy with the experimental data is the position of the peak which we find at 512 nm, whereas experimentally it is located at around 540 nm. This discrepancy is probably because the gold particles do not have exactly a spherical shape. Indeed, Vlieger and co-workers [22–24] have shown that, if instead of spherical particles one considers truncated spherical or oblate spheroidal particles, the plasmon resonance peak is shifted to longer wavelengths. These workers fitted the minimum in the experimental curve to their model and found good agreement assuming particles with a diameter of 26.8 nm and axial ratio equal to 1.21 (truncated spherical model) or with a diameter of 29.4 nm and axial ratio equal to 2.35 (oblate spheroidal model). An extension of our method enabling us to calculate the scattering of electromagnetic waves by non-spherical particles is in progress. Further applications of our method will appear in a forthcoming publication [46].

4. Conclusion

We developed a method for calculating the scattering of light from a periodic two-dimensional array of spherical particles adsorbed on a uniform dielectric slab and demonstrated the applicability of the formalism to real systems. Our first application of the method to the analysis of optical transmission data on a system of gold particles on a sapphire substrate gives a reasonably good account of the experimental situation.

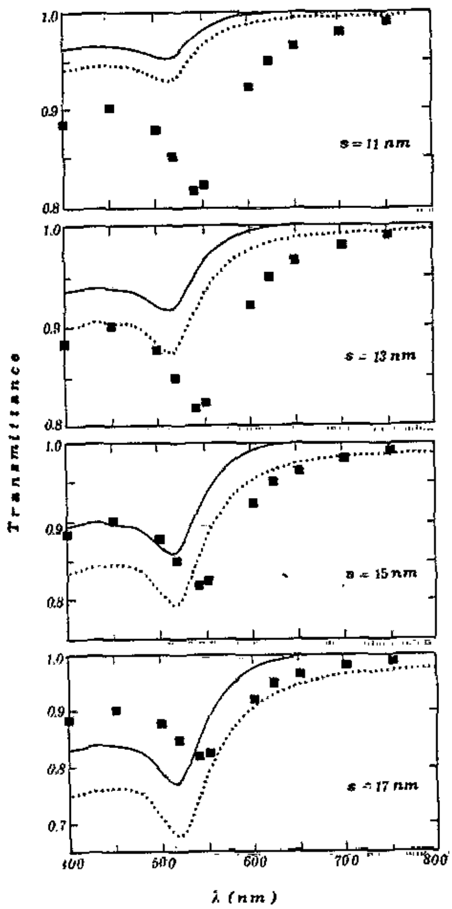

Figure 6. Relative transmittance of a square array of Au spheres on a sapphite substrate with respect to the transmittance of the bare substrate for normally incident light of wavelength λ (———), for various sphere radii S. The lattice constant is equal to 50 nm. The transmittance (. . . .) of the coating array of Au spheres alone and the experimental data (■) are also shown.

Appendix

The matrices $\mathbf{\Omega}^{(1)}$ and $\mathbf{\Omega}^{(2)}$ which describe multiple scattering within a plane of spheres are given by [43]

$$\Omega^{(1)}_{l'm';lm} = [l'(l'+1)l(l+1)]^{-1/2}(2\beta^{m'}_{l'}\beta^{m}_{l} Z^{l'm'-1}_{lm-1} + 2\alpha^{m'}_{l'}\alpha^{m}_{l} Z^{l'm'+1}_{lm+1} + m'mZ^{l'm'}_{lm}) \tag{A1}$$

$$\begin{aligned}\Omega^{(2)}_{l'm';lm} = {} & [l'(l'+1)l(l+1)]^{-1/2}(2l'+1)\{(8\pi/3)^{1/2}(-1)^{m'} \\ & \times \alpha^{m}_{l} Z^{l'-1,m'+1}_{lm+1} B_{l'-1,m'+1}(1,-1;l'm') - (8\pi/3)^{1/2}(-1)^{m'} \\ & \times \beta^{m}_{l} Z^{l'-1,m'-1}_{lm-1} B_{l'-1,m'-1}(1,1;l'm') + mZ^{l'-1,m'}_{lm} \\ & \times [(l'+m')(l'-m')/(2l'-1)(2l'+1)]^{1/2}\}\end{aligned} \tag{A2}$$

where

$$Z^{l'm'}_{lm} \equiv {\sum_{\boldsymbol{R}_n}}' \exp(\mathrm{i}\boldsymbol{k}_{\|}\cdot\boldsymbol{R}_n)\, G_{lm;l'm'}(-\boldsymbol{R}_n) \tag{A3}$$

$$\begin{aligned}G_{lm;l''m''}(-\boldsymbol{R}_n) \equiv {} & \sum_{l'=0}^{\infty}\sum_{m'=-l'}^{l'} 4\pi(-1)^{(l-l'-l'')/2}(-1)^{m'+m''} \\ & \times B_{lm}(l'm';l''m'')h^{+}_{l'}(kR_n)Y_{l'-m'}(-\hat{\boldsymbol{R}}_n)\end{aligned} \tag{A4}$$

$$B_{lm}(l'm';l''m'') \equiv \int Y_{lm}(\hat{r})Y_{l'm'}(\hat{r})Y_{l''-m''}(\hat{r})\,\mathrm{d}\hat{r} \tag{A5}$$

$$\alpha_l^m \equiv \tfrac{1}{2}[(l-m)(l+m+1)]^{1/2} \tag{A6}$$

$$\beta_l^m \equiv \tfrac{1}{2}[(l+m)(l-m+1)]^{1/2}. \tag{A7}$$

The prime on the lattice sum in equation (A3) indicates that the term $\boldsymbol{R}_n = 0$ is to be omitted. We have (see, e.g., [42])

$$Z_{lm}^{l'm'} = 0 \qquad \begin{array}{ll} \text{unless} & l+m \text{ even and } l'+m' \text{ even} \\ \text{or} & l+m \text{ odd and } l'+m' \text{ odd.} \end{array} \tag{A8}$$

From (A8) it follows that

$$\Omega^{(1)}_{l'm';lm} = 0 \qquad \begin{array}{ll} \text{unless} & l+m \text{ even and } l'+m' \text{ even} \\ \text{or} & l+m \text{ odd and } l'+m' \text{ odd} \end{array} \tag{A9}$$

$$\Omega^{(2)}_{l'm';lm} = 0 \qquad \begin{array}{ll} \text{unless} & l+m \text{ even and } l'+m' \text{ odd} \\ \text{or} & l+m \text{ odd and } l'+m' \text{ even.} \end{array} \tag{A10}$$

References

[1] Chang R K and Furtak T E 1982 *Surface Enhanced Raman Scattering* (New York: Plenum)
[2] Ohtaka K and Inoue M 1982 *J. Phys. C: Solid State Phys.* **15** 6463
[3] Inoue M and Ohtaka K 1982 *Phys. Rev.* B **26** 3487
[4] Inoue M and Ohtaka K 1983 *J. Phys. Soc. Japan* **52** 1457
[5] Sievers A J 1979 *Solar Energy Conversion* ed B O Seraphin (Berlin: Springer) p 57
[6] Norrman S, Andersson T, Granqvist C G and Hunderi O 1978 *Phys. Rev.* B **18** 674
[7] Abeles F, Borensztein Y and Lopez-Rios T 1984 *Festkörperprobleme* (*Advances in Solid State Physics*) vol XXIV (Braunschweig: Vieweg) p 93
[8] Craighead H G and Niklasson G A 1984 *Appl. Phys. Lett.* **44** 1134
[9] Niklasson G A and Craighead H G 1985 *Thin Solid Films* **125** 165
[10] Mie G 1908 *Ann. Phys., Lpz.* **25** 377
[11] Debye P 1909 *Ann. Phys. Lpz.* **30** 57
[12] Maxwell Garnett J C 1904 *Phil. Trans. R. Soc.* A **203** 385; 1906 *Phil. Trans. R. Soc.* A **205** 237
[13] David E 1939 *Z. Phys.* **114** 389
[14] Liebsch A and Persson B N J 1983 *J. Phys. C: Solid State Phys.* **16** 5375
[15] Persson B N J and Liebsch A 1983 *Phys. Rev.* B **28** 4247
[16] Agarwal G S and Inguva R 1984 *Phys. Rev.* B **30** 6108
[17] Liebsch A and Gonzales P V 1984 *Phys. Rev.* B **29** 6907
[18] Gomez M, Fonseca L, Rodriguez G, Velazquez A and Cruz L 1985 *Phys. Rev.* B **32** 3429
[19] Vlieger J and Bedeaux D 1980 *Thin Solid Films* **69** 107
[20] Bedeaux D and Vlieger J 1983 *Thin Solid Films* **102** 265
[21] Wind M M, Vlieger J and Bedeaux D 1987 *Physica* A **141** 33
[22] Wind M M, Bobbert P A, Vlieger J and Bedeaux D 1987 *Physica* A **143** 164
[23] Bobbert P A and Vlieger J 1987 *Physica* A **147** 115
[24] Wind M M, Bobbert P A, Vlieger J and Bedeaux D 1989 *Physica* A **157** 269
[25] Doyle W T 1958 *Phys. Rev.* **111** 1067
[26] Doyle W T 1978 *J. Appl. Phys.* **49** 795
[27] Hiltner P A and Krieger I M 1969 *J. Phys. Chem.* **73** 2386
[28] Williams R, Crandall R S and Wojtwitz P J 1976 *Phys. Rev. Lett.* **37** 348
[29] Fujita H and Ametani K 1977 *Japan. J. Appl. Phys.* **16** 1907
[30] Street G B and Greene R L 1977 *IBM J. Res. Dev.* **21** 99
[31] Evans J H 1971 *Nature* **229** 403

[32] Eyre B L and Evans J M 1971 *Void Formed by Irradiation of Reactor Materials* ed S H Pugh *et al* (London: British Nuclear Energy Society) p 323
[33] Mazey D J, Suzan F and Hudson J A 1972 *AERE Report* R7301
[34] Vainstein B K 1966 *Diffraction of X-rays by Chain Molecules* (Amsterdam: Elsevier)
[35] Lamb W, Wood D M and Ashcroft N W 1980 *Phys. Rev.* B **21** 2248
[36] Korringa J 1947 *Physica* **35** 392
[37] Kohn W and Rostoker N 1954 *Phys. Rev.* **94** 1111
[38] Ohtaka K 1979 *Phys. Rev.* B **19** 5057
[39] Ohtaka K 1980 *J. Phys. C: Solid State Phys.* **13** 667
[40] Ohtaka K and Inoue M 1982 *Phys. Rev.* B **25** 677
[41] Inoue M, Ohtaka K and Yanagawa S 1982 *Phys. Rev.* B **25** 689
[42] Pendry J B 1974 *Low Energy Electron Diffraction* (London: Academic) p 121
[43] Modinos A 1987 *Physica* A **141** 575
[44] Jackson J D 1975 *Classical Electrodynamics* (New York: Wiley) p 739
[45] Johnson P B and Christy R W 1972 *Phys. Rev.* B **6** 4370
[46] Stefanou N and Modinos A 1991 *J. Phys.: Condens. Matter* **3** 8149–58